An Enhanced TIMESAT Algorithm for Estimating Vegetation Phenology Metrics From MODIS Data

Bin Tan, Jeffrey T. Morisette, Robert E. Wolfe, Feng Gao, Gregory A. Ederer, Joanne Nightingale, and Jeffrey A. Pedelty

Abstract—An enhanced TIMESAT algorithm was developed for retrieving vegetation phenology metrics from 250 m and 500 m spatial resolution Moderate Resolution Imaging Spectroradiometer (MODIS) vegetation indexes (VI) over North America. MODIS VI data were pre-processed using snow-cover and land surface temperature data, and temporally smoothed with the enhanced TIMESAT algorithm. An objective third derivative test was applied to define key phenology dates and retrieve a set of phenology metrics. This algorithm has been applied to two MODIS VIs: Normalized Difference Vegetation Index (NDVI) and Enhanced Vegetation Index (EVI). In this paper, we describe the algorithm and use EVI as an example to compare three sets of TIMESAT algorithm/MODIS VI combinations: a) original TIMESAT algorithm with original MODIS VI, b) original TIMESAT algorithm with pre-processed MODIS VI, and c) enhanced TIMESAT and pre-processed MODIS VI. All retrievals were compared with ground phenology observations, some made available through the National Phenology Network. Our results show that for MODIS data in middle to high latitude regions, snow and land surface temperature information is critical in retrieving phenology metrics from satellite observations. The results also show that the enhanced TIMESAT algorithm can better accommodate growing season start and end dates that vary significantly from year to year. The TIMESAT algorithm improvements contribute to more spatial coverage and more accurate retrievals of the phenology metrics. Among three sets of TIMESAT/MODIS VI combinations, the start of the growing season metric predicted by the enhanced TIMESAT algorithm using pre-processed MODIS VIs has the best associations with ground observed vegetation greenup dates.

Index Terms—MODIS, NACP, phenology, TIMESAT.

I. INTRODUCTION

L AND surface phenology is defined as the seasonal pattern of variation in vegetated land surfaces observed from remote sensing. Because the seasonal pattern of vegetation is sensitive to small variations in climate, phenological records can be a useful proxy in the study of climate change. Land surface phenology is distinct from the traditional definition of phenology, which is the study of the times of recurring natural phenomena, i.e., the date of emergence of leaves and flowers, and the date of leaf coloring and fall in deciduous trees (http://www.usanpn.org/). The traditional definition refers to specific life cycle events using *in situ* observations of individual plants or species, while land surface phenology observed from remote sensing is aggregated information at the spatial resolution of satellite sensors [1]. The Advanced Very High Resolution Radiometer (AVHRR) series is the first set of satellite sensors that have a frequent repeat cycle and synoptic information suitable to monitor land surface vegetation phenology across large areas [2]. The Moderate Resolution Imaging Spectroradiometer (MODIS) provides a more comprehensive data source to study land surface phenology at continental and global scales. The two MODIS sensors are key instruments aboard NASA's Terra and Aqua satellites. Each MODIS sensor observes the entire Earth's surface every one to two days and provides land surface information at scales useful for studying land surface processes (250 m to 1 km).

Developing algorithms to automatically retrieve land surface phenology metrics from satellite data has been a popular research topic for the last decade. However, the nature of satellite data makes it difficult to extract phenological metrics from it directly. First, satellite data are noisy due to variations in viewing and illumination geometry, sky and cloud properties, and surface conditions. Second, there are absences of vegetation information due to clouds, snow, and other effects such as atmospheric aerosols. Therefore, time-series satellite data are commonly quality-screened and/or smoothed to minimize noise and compensate for the absence of data before phenological metrics can be estimated. Various methods have been developed to estimate phenology metrics based on the time series of remotely sensed vegetation index (VI), from simple linear smoothing window methods [3], [4] to more complicated analytical curve function methods [4]–[6]. After smoothing the dataset, most of the algorithms have used a prescribed threshold over the time series to define the start and the end of the growing season [2], [3], [7]. Some algorithms use an analytical indicator to define the start and end of the growing season, e.g., maximum curvature rate of fitted logistic curve [5].

We enhanced the TIMESAT program to develop a phenology retrieval algorithm. TIMESAT was developed by Jonsson and Eklundh [4] for analyzing time-series satellite sensor data. The advantages of this program are: a) it is open source software, b) it provides three different smoothing functions to fit time-series data: asymmetric Gaussian, double logistic and adaptive Savitzky–Golay filtering, c) a user-defined weighting scheme is

applicable in the smoothing process, and d) a comprehensive set of phenology metrics is generated from the smoothed time series satellite data.

Gao *et al.* [8] revised the TIMESAT software to produce temporally smoothed and spatial gap-filled MODIS Normalized Difference VI (NDVI) and Enhanced VI (EVI) products. The NDVI and EVI are calculated from 8 day composite MODIS Terra surface reflectance products (MOD09Q1 and MOD09A1) at 250 m and 500 m resolution [9], [10]. When calculating 250 m resolution EVI, the 500 m blue band is extrapolated from 500 m resolution to 250 m resolution. Our research is based on the revised TIMESAT software of Gao *et al.* [8] and makes additional improvements to retrieve MODIS phenology metrics based on MODIS time-series VI datasets.

In this paper, we describe further improvements in our TIMESAT-based phenology retrievals. We use EVI as an example to compare the phenology metrics retrieved from three sets of TIMESAT/MODIS VI combinations: 1) the original TIMESAT algorithm with the original EVI, 2) the original TIMESAT algorithm with pre-processed EVI, and 3) the enhanced TIMESAT and pre-processed EVI. Finally, we assess the association between retrieved vegetation greenup dates and ground observations.

II. METHODOLOGY

A. Selection of the Smoothing Function

There are three smoothing functions available in TIMESAT software: adaptive Savitzky–Golay filtering, asymmetric Gaussian, and double logistic. The adaptive Savitzky–Golay filtering approach uses local polynomial functions. It can capture subtle and rapid changes in the time-series but is also sensitive to noise. Both asymmetric Gaussian and double logistic approaches use semi-local methods. Less sensitivity to the noise tends to provide a better description of the beginning and end of the growing season. Gao *et al.* [8] found that both asymmetric Gaussian and double logistic approaches in the TIMESAT program produced similar results, with the exception of the asymmetric Gaussian method, which is less sensitive to the incomplete time-series data. This is a significant advantage considering many missing data or poor quality dataexist in satellite observations due to snow, clouds, shadow, and very low sun angle. Therefore, the asymmetric Gaussian method was selected for temporally smoothing data and estimating phenology metrics. The base function of asymmetric Gaussian is

$$g(t, x_1, x_2, \ldots, x_5) = \begin{cases} \exp\left[-\left(\frac{t-x_1}{x_2}\right)^{x_3}\right] & \text{if } t > x_1 \\ \exp\left[-\left(\frac{x_1-t}{x_4}\right)^{x_5}\right] & \text{if } t < x_1 \end{cases}.$$

(1)

For this function, x_1 determines the position of the maximum or minimum with respect to the independent time variable t, while x_2 and x_3 determine the width and flatness (kurtosis) of the function for values greater than x_1 (the right-hand side or second half of the season). Similarly, x_4 and x_5 determine the width and flatness of the left side (or first half of the season). The details of the algorithm can be found in [4] and [8].
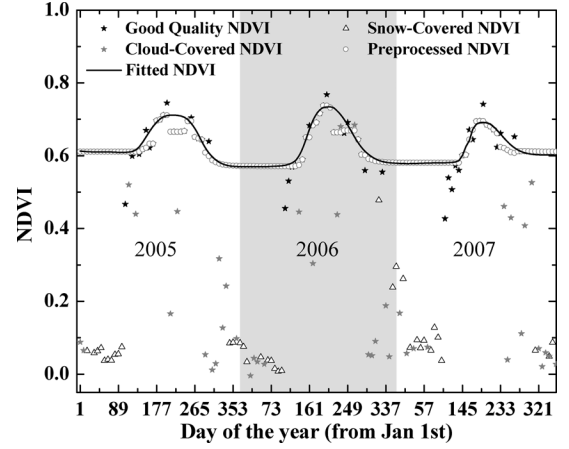

Fig. 1. An example of smoothing and gap-filling MODIS NDVI data for the three-year period 2005–2007. The selected 500-m resolution pixel is in tile h12v04. The applied smoothing function is the asymmetric Gaussian function [2].

B. Preprocess VI: Eliminating Noise and Filling the Winter Data Gap

Fig. 1 shows the temporal trajectory of EVI from 2005 to 2007 of a pixel located in the Harvard Forest, USA (from MODIS tile h12v04 [15]). The time-series data clearly contains some noise due to variations in viewing and illumination geometry, sky and cloud properties, and snow cover. Some of this can be removed by eliminating the values for which the quality assessment (QA) indicates poor pixel quality [11]. Excluding the poor quality data in the curve fitting progress improves the retrieval quality. However, the temporal curve is not retrievable when there is missing or poor quality data. The threshold of the retrievable data gap, a parameter in the TIMESAT software, is four months if there is one growing season within a year, and two months if there are two growing season within a year. When the data gap is larger than the threshold, greenup and/or browndown, information could be missing from the time series and the fitted curve would not be accurate. However, if the data gap occurs in the non-growing season (e.g., winter), when the vegetation reflective characteristics should remain relatively constant, the curve fitting process should still be performed. In our approach, to define the winter season, we utilize: 1) the snow flag embedded in the QA information for the MODIS surface reflectance product (MOD09A1) and 2) the 8-day composite MODIS Land surface temperature product (MOD11A2) [16], [17]. The winter season is defined as a period which is longer than half a month when a pixel is snow-covered or the night land surface temperature is equal to/or below 0 °C (also known as a frost day). Many of the biochemical processes of vegetation are sensitive to low temperature [18]. The photosynthesis of vegetation increase quickly once the temperature exceeds the minimum temperature threshold. Different ecosystems have different minimum temperature thresholds. For example, the threshold for northern spruces and pines is −1 °C [19], while the threshold for tropical trees is 0 °C [20]. The minimum temperature threshold ranges from −2 °C to 5 °C [21], [22]. It is impossible to assign the minimum temperature threshold for each ecosystem in the continental/global scale. Therefore, we
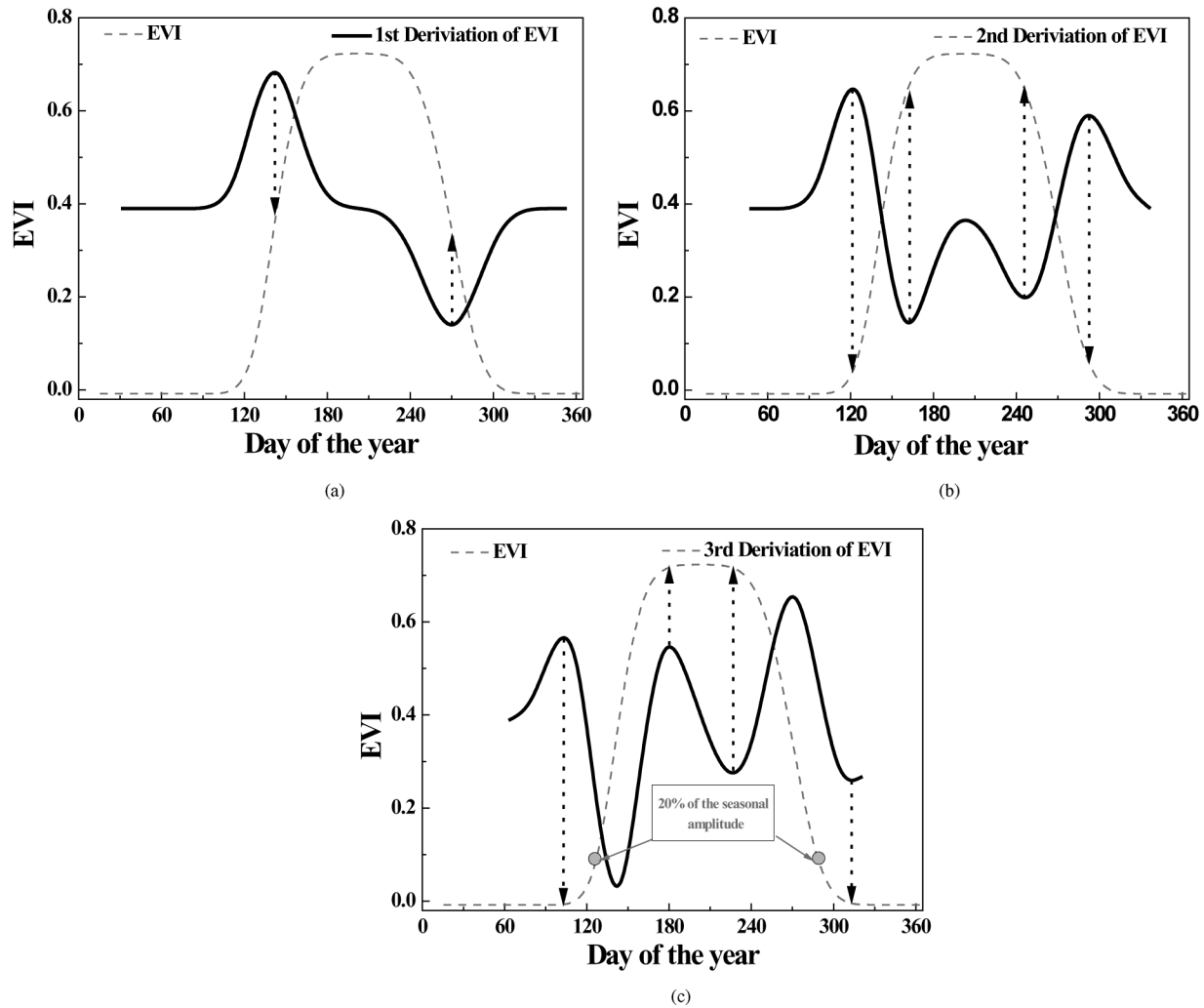
Fig. 2. An example of the biophysical information extracted by first, second, and third derivative of time series EVI curve.

use 0 °C as a universal threshold to help defining the growing season. A smoothed flat curve is used to connect the latest growing season point and the first growing season point of the next growing season. Then these revised data are fitted with a Gaussian curve (Fig. 1).

C. Improved Method for Determining Phenology Dates

To improve the accuracy of estimating phenology dates, we first revised the TIMESAT algorithm to incorporate ancillary information (the snow-cover flag and land surface temperature from MODIS data products, Section II-B). In the original TIMESAT software, the key phenology dates are identified with a threshold method (the default value is 20% of the seasonal amplitude, Fig. 2(c)) measured from the left or right minimum level. The advantage of this method is that it is easy to tune the threshold according to the local conditions. However, there is no underlying biophysical meaning for the threshold and a single threshold value may not be suitable for different locations and/or different species. We are producing phenology data sets at the continental scale and require a more robust and objective approach to retrieve key phenology dates for a wide range of ecosystem types.

The derivative of the time-series data can be used to identify the change of state, such as the start/end of greenup[5]. We investigated the derivatives of VI time-series data and selected the third derivative as the indicator for best indentifying phenology dates. Fig. 2 shows the temporal trajectory of EVI and the first, second, and third derivative of EVI for a pixel in the Harvard Forest in 2006. The local maximum and minimum of the first derivative curve corresponds to the maximum rate of increase and decrease of the corresponding greenup and browndown processes. The local maximum and minimum of the second derivative curve corresponds to the beginning of the greenup, end of greenup, peak growing season, beginning of the browndown, and end of browndown, respectively. The local maximum and minimum of the third derivative curve corresponds to the beginning of greenup, maximum increasing slope, end of greenup, beginning of browndown, maximum decreasing slope, and end of browndown.

Both the second and third derivative curves retrieve the timing of the greenup and browndown, as marked in Fig. 2(b) and (c), respectively. The beginning of greenup detected by the second derivative curve represents the timing when the majority of vegetation within the pixel is turning green. The beginning of
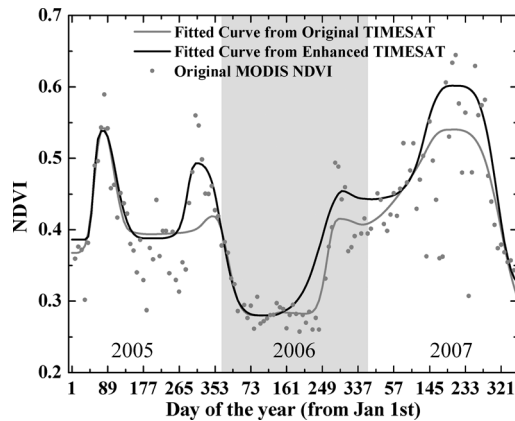
Fig. 3. An example of fitted NDVI curve over unevenly distributed growing seasons. This sample pixel locates in Southwest US (within tile h09v06). The data period is 2005–2007.

greenup detected by the third derivative curve selects the point on the fitted curve where the change of the greenup rate is the greatest. We chose the third derivative curve because the timing is at the very beginning of the change in VI, representing the first flush of greenness on the ground. This agrees with the definition of "beginning of greenup" normally used by the ground observations, in which the first green leaves appear. The same reasoning was used to select the third derivative curve to detect the end of greenup, the beginning of browndown, and the end of browndown.

D. Retrieving Unevenly Distributed Growing Seasons

To retrieve phenology metrics for one calendar year, three years of data are required, including the one year prior to and after the year of interest (Fig. 1). All growing seasons within the three-year period are retrieved, but only the growing season(s) of the middle year are recorded. The original TIMESAT algorithm assumes the growing season starts and ends at a similar time annually. It tries to locate the growing season for the second year in the same time period as the first and third years. However, it is not always the case especially for semi-arid regions where the growing seasons are driven by the precipitation. For example, in Fig. 3, the original TIMESAT tries to locate a growing season at the middle year around days 73 to 161. It was not successful because the initial flush of greenness in the second year (2006) is not present perhaps due to drought or fire.

We made three improvements to capture unevenly distributed growing seasons. First, we fit the Gaussian curve twice over the original MODIS VI. The weight of high quality VI is enhanced if they are not fitted during the first algorithm iteration [8]. Secondly, we re-defined the start/end of growing season according to the Gaussian curve from the first fit iteration. We do not assume even distribution of the growing season over the three years, but define the start/end of the growing seasons according to the maximum and minimum VIs over the entire period. Thirdly, the enhanced algorithm examines the start and end of all growing seasons, then records the first two growing seasons, which occur in the second year of the three-year time series. Each growing season is considered as occurring in the second year if it begins within the second year and ends by

the end of the third year. In the sample pixel shown in Fig. 3, the enhanced TIMESAT algorithm captures the growing season, which spans the second and third years. The recorded growing season begins in the second year around day 300 (this example pixel is from the Southwest US at latitude 28.21, longitude. −99.46. The annual rainfall from a weather station in Encinal, Texas, about 14 miles southeast, indicated annual rainfall for 2005–2007 as: 20.45, 10.59, 29.89 inches. This supports the notion that a phenology algorithm needs to allow for year-to-year variability).

E. Gap-Fill Phenology Retrievals

The phenology data set includes 25 phenology parameters and 3 ancillary parameters [Table I]. The first 11 parameters are included in the original TIMESAT software. There are up to two data layers for each parameter, corresponding to the first two detected growing seasons. The remaining six parameters are provided as additional information related to the pixel or time series data.

For a small fraction of the pixels, the temporally fitted annual VI curve is not derived because there are insufficient high quality values. For these pixels, Gao *et al.* [8] developed a spatial gap-filling approach. In this case, the data are gap-filled by referencing an annual curve from a neighboring pixel with the same land cover type. The seasonal variation of the referenced curve is adjusted to fit the sparse high-quality observations and substitute the missing and low quality observations. Then the high-quality and substituted observations are used to refit an annual VI curve from which the phenology metrics are estimated. A benefit of this spatially smoothed and gap-filled algorithm is that the spatial coverage of this phenology dataset is greatly improved.

The enhanced TIMESAT algorithm has been applied to retrieve phenology metrics from both MODIS EVI and NDVI. Fig. 4 shows the greenup and browndown dates estimated using this approach over North America for 2006. Fig. 5 shows the data density contour of greenup and browndown date in dateEVI – dateNDVI space. More than 50% of the pixels have similarly retrieved greenup/browndown dates from EVI and NDVI. The difference emerges in Midwest and Southwest US, and Florida. The Midwest and Southwest are semi-arid regions, while Florida is dominated by green vegetation. In these regions, the signal of the growing season is not distinct where either the growing season is very short or the magnitudes of VI changes during the growing season are very small. From Fig. 5, the difference between browndown date is more than the difference between greenup date. This is because the browndown is a more gradual progress than greenup, which makes it easier to determine.

The difference between phenology dates retrieved from EVI and NDVI is negligible compared with the difference between phenology dates from the original and enhanced TIMESAT. Here, we use EVI as an example to compare the phenology metrics retrievals from the original and enhanced TIMESAT. It should be noted that the phenology metrics retrieved from NDVI show similar differences between original and enhanced TIMESAT. However, we do not present NDVI results here to reduce the redundancy.

TABLE I
LIST OF BIOPHYSICAL PARAMETERS INCLUDED IN MODIS PHENOLOGY PRODUCT

Name	Description	Unit
Greenup Date	At the beginning of the growing season, time for which the vegetation index begins to increase	Day from Jan 1st
Browndown Date	At the end of the growing season, time for which the vegetation index ends to decrease	Day from Jan 1st
Season Length	Time from the start to the end of the season	Day
Base Level	Given as the average of the left and right minimum VI values	VI unit
Peak Date	Computed as the mean VI value of the time for which, respectively, the greenup process ends and browndown process begins	Day from Jan 1st
Max Peak Value	Largest VI value for the fitted function during the season	VI unit
Amplitude	Difference between the maximum VI value and the base level	VI unit
Greenup Rate	Calculated as the difference between the VI values evaluated at the beginning and ends of greenup process divided by the corresponding time difference	VI unit per 8 days
Browndown Rate	Calculated as the difference between the VI values evaluated at the beginning and ends of browndown process divided by the corresponding time difference	VI unit per 8 days
Large Integrals	Integral of the function describing the season from the season start to the season end	VI unit
Small Integrals	Integral of the difference between the function describing the season and the base level from season start to the season end	VI unit
Annual Maximum Value	Largest VI value for the fitted function during the year	VI unit
Annual Minimum Value	Smallest VI value for the fitted function during the year	VI unit
Annual Mean Value	Mean VI value for the fitted function over the year	VI unit
RMSE	RMSE (Root Mean Square Error) value between high quality original VI data and corresponding fitted VI data	N/A
Quality Flag	An indicator on the quality of retrieved phenology metrics or why the pixel is failed to retrieve.	N/A
Landcover	Landcover type in IGBP scheme	N/A

The first eleven parameters are from original TIMESAT software. There are two data layers for each parameter, corresponding to the first two detected growing seasons. The remaining six parameters are added for the user's convenience. There is one data layer for each parameter.

F. Evaluation of the TIMESAT Algorithm Improvements

To evaluate the improvements described above, we compared three sets of TIMESAT and MODIS EVI combinations: a) Original EVI and Original TIMESAT (OO), b) Preprocessed EVI and Original TIMESAT (PO), and c) Preprocessed EVI and Enhanced TIMESAT (PE). MODIS EVI is at 500 m resolution. The study region covers the middle and eastern US (Fig. 4(a)) with a focus on four specific MODIS tiles: (1) h12v04, (2) h11v05, (3) h09v06, and (4) h08v06 (Fig. 4(c)) [15]. Tile 1, over the New England region, represents an area with a strong growing season and a long period of snow cover. Tile 2 represents an area with a strong growing season signal and little, if any, snow cover. Tile 3 includes Southwest Texas and Eastern Mexico covering semi-arid and non-arid areas. Here the temporal distribution of the growing seasons is complex, especially in the boundary region between semi-arid and non-arid regions. Tile 4, over Mexico, represents the growing season characteristic of a semi-arid region.

III. RESULTS AND DISCUSSION

Fig. 6 shows the dependence of greenup and browndown dates on latitude for different land cover types across the middle and eastern US between 30°N and 50°N. The figure was created by computing average dates for greenup for one

degree increment of latitude, stratified by land cover classes provided by the Collection 4 MODIS land cover product [12]. The progressively later greenup dates and earlier browndown dates from south to north are consistent with known vegetation phenology characteristics. At lower latitudes (30°N to 40°N), snow cover is less prevalent through winter. Therefore, the snow flag and land surface temperature are less frequently used to define the growing season. The greenup and browndown dates estimated from the original TIMESAT algorithm (OO and PO) agree very well. However, at this lower latitude, the enhanced TIMESAT algorithm (PE) reports earlier greenup and later browndown dates. This is due to the use of the third derivative method to define phenology dates (see Section II-C). In mid to high latitude regions (40°N to 50°N), the latitudinal dependence of greenup dates is apparent. However, the browndown dates from OO and PO shows less latitude dependence than the PE algorithm (e.g., deciduous forest between 45°N and 50°N, crops between 40°N and 45°N, and grasslands between 45°N and 50°N). For the crop and grasslands cover types at high latitude, we see some spurious and unexpected variation in the browndown dates for the OO and PO algorithms with respect to latitude. This is likely due to the fact that neither algorithm is accounting for snow cover or land surface temperature. Fig. 6 shows that the phenology dates retrieved from
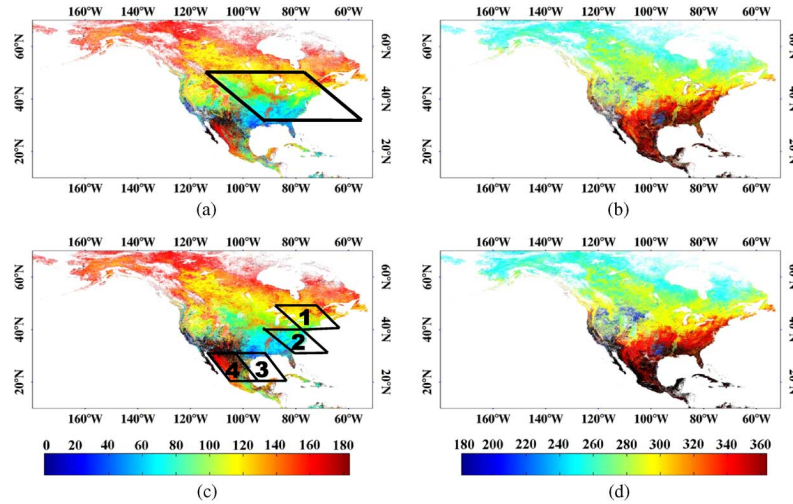
Fig. 4. The days of greenup and browndown derived from 500 m resolution MODIS EVI and NDVI over North America in 2006. The black box in panel (a) marked the area where we performed the latitude-dependence analysis. The black boxes mark the four tiles, (1) h12v04, (2) h11v05, (3) h09v06, and (4) h08v06, where we perform detailed analyses. (a) $\mathrm{Greenup_{EVI}}$. (b) $\mathrm{Browndown_{EVI}}$. (c) $\mathrm{Greenup_{NDVI}}$. (d) $\mathrm{Browndown_{NDVI}}$.
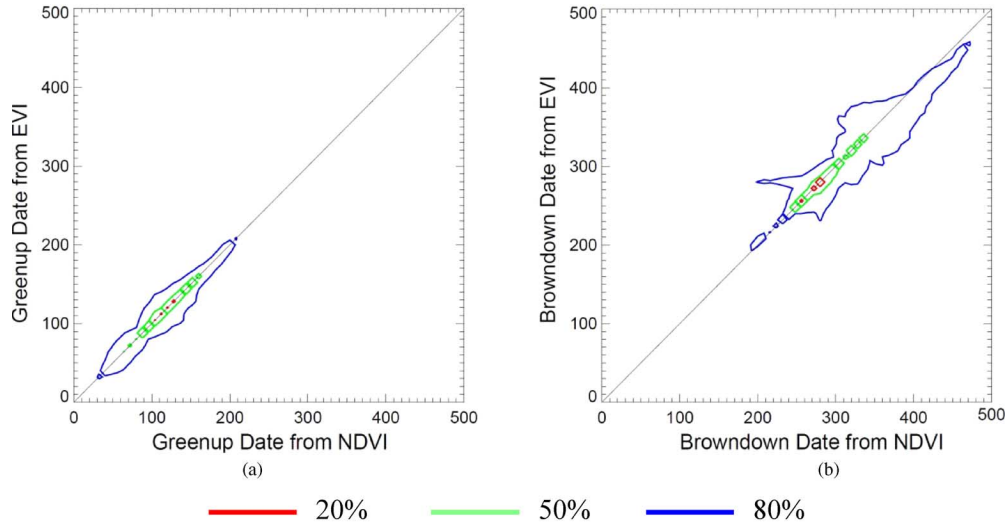

Fig. 5. Data density contour of greenup (a) and browndown (b) date in date–from-NDVI-EVI space. The space enclosed by the red line contains 20% data, while the green and blue lines correspond to 50% and 80% density, respectively.

enhanced TIMESAT algorithm, which incorporates the snow flag and land surface temperature, exhibit a more reasonable latitudinal dependence than the phenology dates estimated from original TIMESAT algorithm (OO and PO).

We employ a retrieval ratio to describe the spatial coverage of the land pixels with estimated phenology metrics. Overall, PE exhibits the highest spatial coverage (or retrieval ratio) among three sets of algorithm/MODIS data combinations. The retrieval ratio varies from one region to another. Fig. 7 presents the retrieval ratio of the four MODIS tiles selected for discussion. In Tile 1, the retrieval ratio of OO is only 43% while PO and PE are both above 99%. This is due to the long snow-covered period in the North Eastern US. The snow-covered pixels are considered poor quality and will not be applied in curve fitting. Here OO failed because of a lot of data was either poor quality or missing, while PO and PE succeeded because missing values within the non-growing seasons are filled in the preprocess step (Section II-A and Fig. 2). In all other tiles, there is little or no

snow cover. Therefore, all three algorithm/MODIS combinations perform well with similar retrieval ratio. For tile 3, the retrieval ratio of PE is about 5% higher than OO and PO. This is due to the complex growing season pattern at the boundary of semi-arid and non-arid region (Fig. 4). Here PE's successful retrieval is a result of the second fitting process and adjusted growing season positions (Section II-D).

Fig. 8 presents histograms of the pair-wise differences in phenology dates retrieved from three sets of TIMESAT/MODIS data combinations. Considering the different retrieval ratios (Fig. 7), Fig. 8 only includes the region where all three sets report phenology metrics. In general, the phenology dates from OO and PO methods agree well, while PE reports earlier greenup dates and later browndown dates. This is due to the different method used to define greenup and browndown dates. OO and PO are using 20% of the seasonal amplitude as the threshold. The positions selected by the 20% threshold are within the very beginning and end of the growing season,
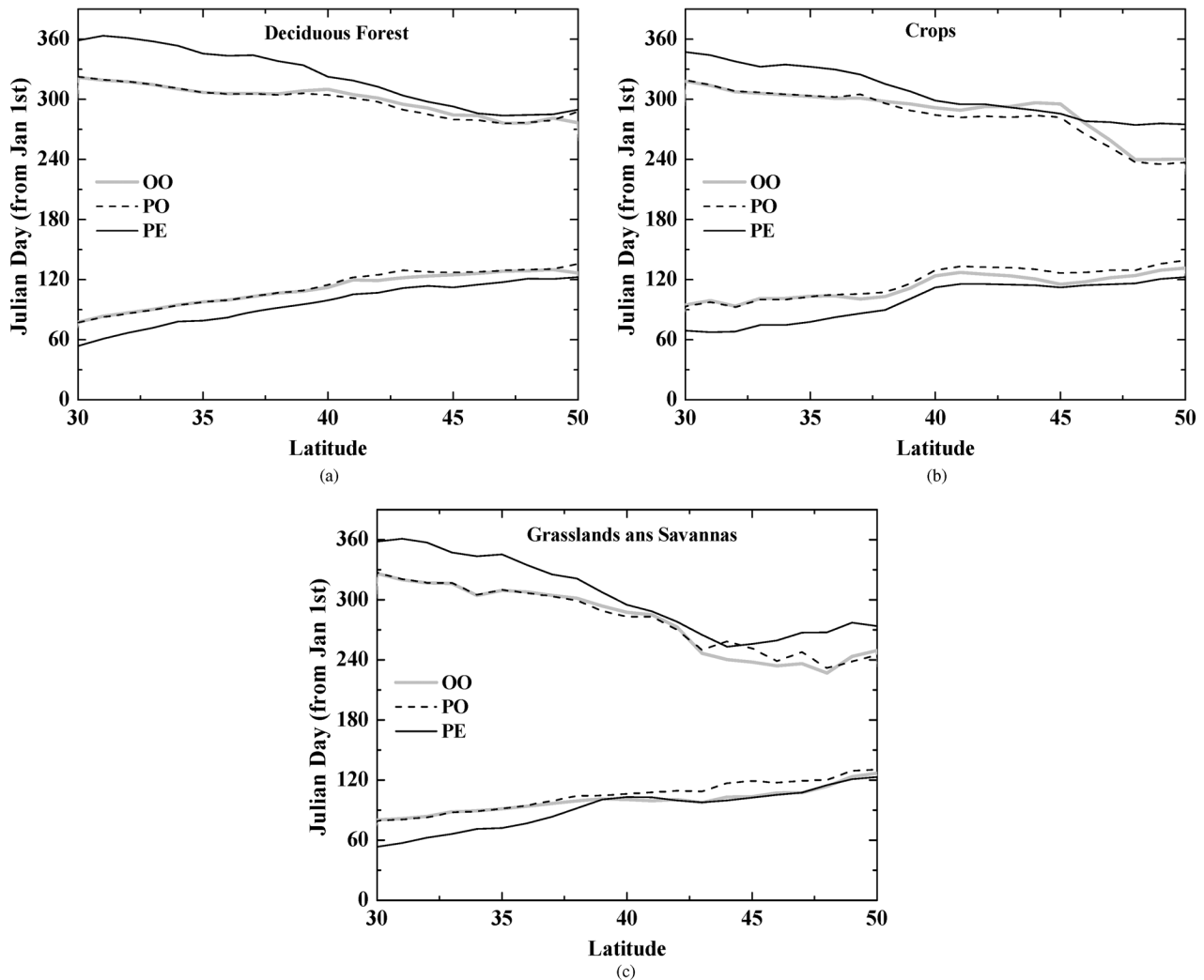
Fig. 6. MODIS 500 m EVI greenup (earlier) and browndown (later) dates averaged every 1 degree of latitude for the main landcover types for the six MODIS tile region in Fig. 4(a) using the (a) OO, (b) PO, and (c) PE methods.

which are defined by the third derivative (Fig. 2(c)). This date difference also depends on how quickly the EVI changes during greenup and browndown. For example, the greenup in Fig. 2(c), 20% amplitude is achieved later if the EVI changes slower, while the greenup date determined by the third derivative is relative stable no matter EVI changing quicker or slower. Therefore, a quicker change leads to a smaller difference between phenology dates captured by 20% amplitude and the third derivative method and vice versa. Vegetation normally changes more quickly during greenup than browndown. Therefore, the difference between enhanced TIMESAT and original TIMESAT is much smaller in greenup than in browndown (Fig. 8).

Finally, the association between the estimated greenup dates and ground observations was assessed. The ground observations are provided by various projects, including the Chequemegon Ecosystem Atmosphere study, Global Learning and Observations to Benefit the Environment (GLOBE), Harvard Forest Long Term Ecological Research (LTER), Howland Research Forest, Long Lake Conservation Center, Prairie Westlands Learning Center, and Rocky Mountain Biological Laboratory
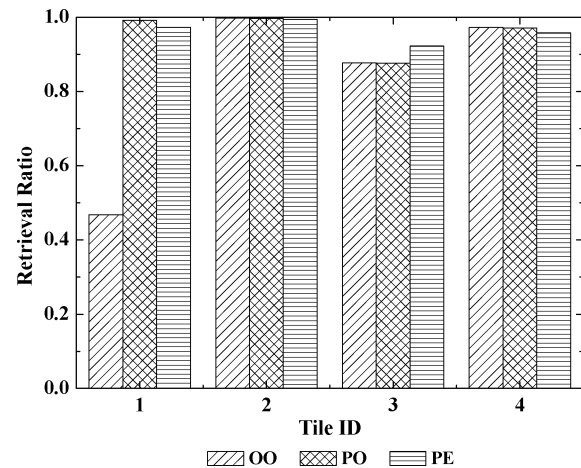

Fig. 7. Successful retrieval ratio of OO, PO, and PE algorithms over study tiles.

(Table II). The first two projects report greenup dates for two and five sites respectively, while other projects report phenology events at a single site. It should be noted that not all
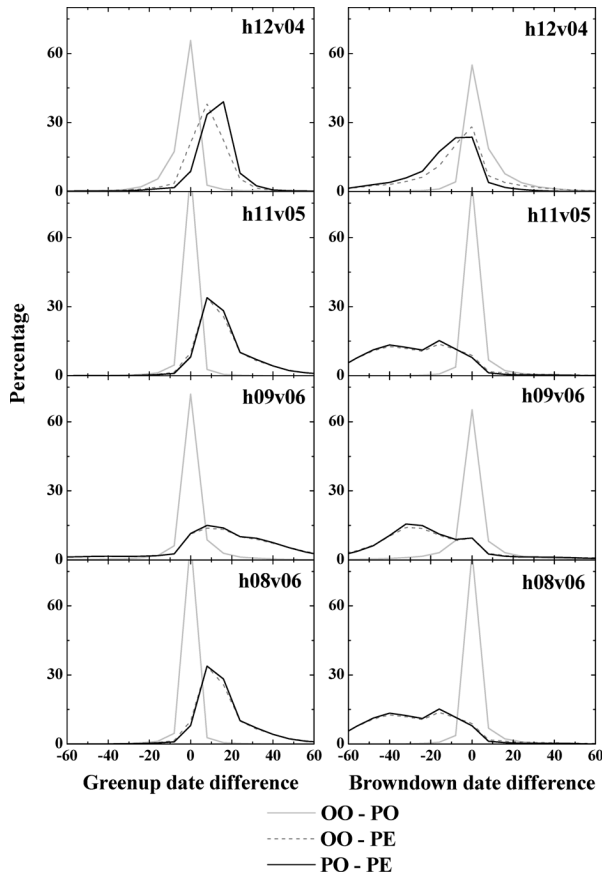
Fig. 8. Histograms of difference of phenology dates derived from OO, PO, and PE over 500 m EVI.

projects record first flush of the leaves. The Long Lake Conservation Center and Prairie Westlands Biological Laboratory records include many phenological events, e.g., flowing time, animal migration etc., but without the record of greenup. For Long Lake Conservation Center, the phenology diary records consist of "Ice completely gone off Long Lake" on April 10, "60 degree outside" on April 11, and "Red maples blossom" on April 15. We considered these phenomena related to the timing of greenup. We selected the April 11 as the greenup date (60 degree outside) for this site. For Prairie Wetlands Learning Center, the phenology diary reports consist of "western chorus frogs singing in center pond" on April 5th, and "pasque flowers blooming" on April 12th. The first event presents the timing of the complete ice melt. The second event presents the timing of appearance of green leaves. Therefore, we selected April 5th as the greenup date for this site. The inaccuracy of greenup dates of these sites should be within 7 days, which does not lead to a significant change in the comparison with retrieved greenup dates from satellite data. Fig. 9 shows the association between estimations and ground observations. OO has the least valid retrievals ($n = 8$) over ground observation sites and the weakest correlation ($R^2 = 0.21$). Four of twelve sites are not successfully retrieved due to the long snow-covered period. PO and PE have successful retrievals over all ground observation sites ($n = 12$), while PE's retrievals have better correlation ($R^2 = 0.65$) with ground observations than PO's estimations

($R^2 = 0.29$). The root mean square error (RMSE) for OO, PO, and PE are 23.5, 23.1, and 11.1, respectively. The average of the bias (defined as the difference between estimated and observed greenup dates) for OO, PO, and PE results are 14.4, 9.4, and 0.3 days. OO and PO tend to report later greenup dates than ground observations, while PE results do not have significant bias comparing with ground observations. This is due to the difference on how to determine greenup dates. The default 20% amplitude threshold, used by OO and PO, presents the ground situation when most of the leaves are at bud break. This usually happens later than the greenup date recorded by the ground observers, who normally note the first leaves at bud break which represents the start of photosynthetic activity. The design of the third derivative method is to detect the first appearance of green leaves. This is more representative of the criteria of ground observers.

IV. CONCLUSIONS

This paper described a vegetation phenology estimation algorithm based on preprocessed MODIS data and the enhanced application of the TIMESAT software. This algorithm is one of several that have been developed to estimate phenology metrics using MODIS data. It has been used to produce 250 m and 500 m resolution in North America annual phenology metrics based on MODIS EVI and NDVI. The datasets are freely available through the web-based distribution system (http://accweb.nascom.nasa.gov) together with 500 m resolution (based on MODIS EVI and NDVI) and 1 km resolution phenology products from 2000–2007 based on the MODIS LAI product (following the same algorithm presented here). Processing options include mosaicing of multiple MODIS tiles, reprojecting the products to a regional grid, subsetting the products spatially and by parameter, aggregating the products spatially, and selecting two options for file (HDF or GeoTIFF).

We improved the TIMESAT algorithm by incorporating ancillary information, snow-cover flag and land surface temperature, from MODIS data products. Through comparing the phenology metrics retrieved from original and enhanced TIMESAT software, we found that enhanced TIMESAT software has a higher overall successful retrieval ratio and better geographically and ecologically realistic estimates of phenology events than the original TIMESAT software. A simple assessment of the association between greenup dates from original and enhanced TIMESAT indicates satisfactory result from enhanced TIMESAT.

Validation is a vital step for calibrating remote sensing based scientific algorithms [13]. However, validating phenology metrics derived from moderate or coarse resolution satellite data product is difficult due to the scale-mismatch with ground observations as well as vegetation heterogeneity. Vegetation is rarely uniform at the scale of MODIS resolution, while field observations normally indentify the timing of the budburst or flowering for one or a few plants at each validation site. The relationship between observed phenology events and the average vegetation phenology status over the spatial coverage of the MODIS pixel are usually not quantitatively assessed. For example, the budburst timing of observed plants could be a few days earlier or later than other plants within the MODIS pixel.
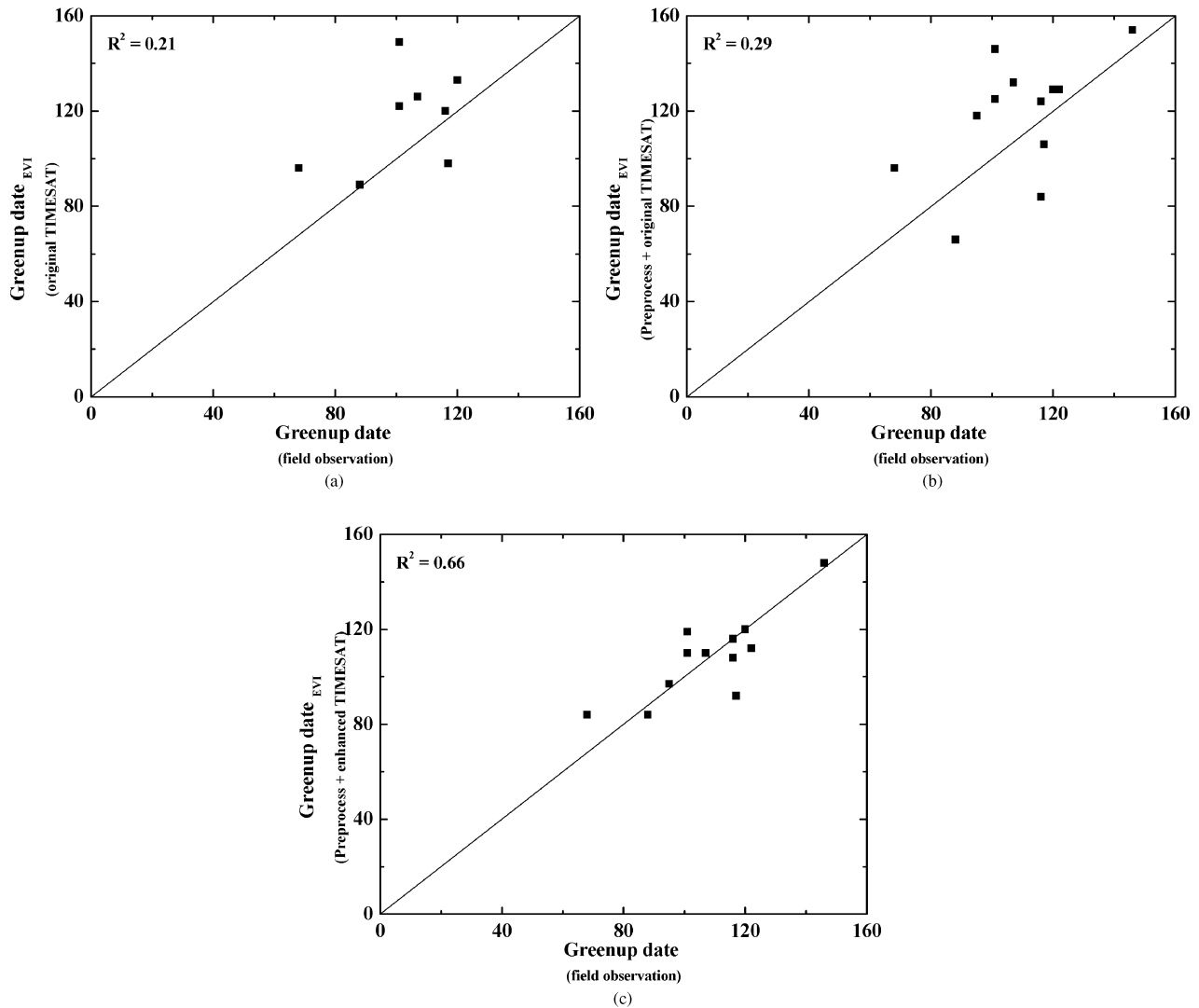
Fig. 9. Comparison between field-observed greenup dates and greenup dates derived from MODIS 500 m EVI using the (a) OO, (b) PO, and (c) PE methods.

TABLE II
VALIDATION SITES AND THE FIELD OBSERVED EVENTS, WHICH ARE CONSIDERED AS THE TIMING OF GREENUP

Site/Network Name	Site Numbers	Observed Events
Chequemegon Ecosystem Atmosphere Study	2	First Appearance of leaves
GLOBE	5	First Appearance of leaves
Harvard Forest LTER	1	First Appearance of leaves
Howland Research Forest	1	First Appearance of leaves
Long Lake Conservation Center	1	First report of land surface temperature > 60° F
Prairie Westlands Learning Center	1	First report of Chorus Frogs and Trumpeter Swans
Rocky Mountain Biological Laboratory	1	First Appearance of leaves

Another obstacle is the quality of the ground data depends on the experience of the data collector. The collection of the phenology dates on the ground is different from collection of other biophysical parameters, such as NDVI and Leaf Area Index (LAI), and is often dependent on the subjective decision of the data collector. For the same validation site, different data collectors could give different phenology dates. Some may report a few days earlier greenup dates, and the others may report a few days later greenup dates. This depends on the data collector's experience and knowledge although protocols for ground collection being implemented by USA National Phenology Network (NPN).

Though various field programs are collecting phenological information, most of them are recording specific species or events not directly related to vegetation status. For example, two ground observations in Table II are not directly vegetation status (one is based on temperature and one is based on observing frogs or swans). Despite this, we utilized these two

data sets as they are considered to be closely associated with the timing of vegetation greenup.

Finally, phenological metrics derived from NDVI and EVI are not in 100% agreement with each other [14]. We are still exploring which vegetation index is the best for presenting the phenological phase. Also, we are working with the Land Product Validation subgroup within the committee on Earth Observing Satellite (CEOS) to continue an international effort to improve both the reference data and methods available for the validation of land surface phenology products (http://lpvs.gsfc.nasa.gov/).

REFERENCES

[1] B. Reed, M. D. Schwartz, and X. Xiao, *Remote Sensing Phenology: Status and the Way Forward, in Phenology of Ecosystem Process*, A. Noormets, Ed. New York: Springer, 2009, p. 275.

[2] M. A. White, P. E. Thornton, and S. W. Running, "A continental phenology model for monitoring vegetation responses to interannual climatic variability," *Global Biogeochem. Cycles*, vol. 11, pp. 217–234, 1997.

[3] D. Lloyd, "A phenological classification of terrestrial vegetation cover using shortwave vegetation index imagery," *Int. J. Remote Sens.*, vol. 11, pp. 2269–2279, 1990.

[4] P. Jonsson and L. Eklundh, "TIMESAT—A program for analyzing time-series of satellite sensor data," *Comput. Geosci.*, vol. 30, pp. 833–845, 2004.

[5] X. Zhang, M. A. Friedl, C. B. Schaaf, A. H. Strahler, J. C. F. Hodges, F. Gao, B. C. Reed, and A. Huete, "Monitoring vegetation phenology using MODIS," *Remote Sens. Environ.*, vol. 84, pp. 471–475, 2003.

[6] T. Roetzer, M. Wittenzeller, H. Haechel, and J. Nekovar, "Phenology in central Europe – differences and trends of spring phenophases in urban and rural areas," *Int. J. Biometeorol.*, vol. 44, pp. 60–66, 2000.

[7] R. B. Myneni, C. D. Keeling, C. J. Tucker, G. Asrar, and R. R. Nemani, "Increased plant growth in the northern high latitudes from 1981–1991," *Nature*, vol. 386, pp. 698–702, 1997.

[8] F. Gao, J. T. Morisette, R. E. Wolfe, G. Ederer, J. Pedelty, E. Masuoka, R. Myneni, B. Tan, and J. Nightingale, "An algorithm to produce temporally and spatially continuous MODIS-LAI time series," *IEEE Trans. Geosci. Remote Sens. Lett.*, vol. 5, pp. 60–64, 2008.

[9] E. F. Vermote, N. Z. El Saleous, and C. O. Justice, "Atmospheric correction of MODIS data in the visible to middle infrared: First results," *Remote Sens. Environ.*, vol. 83, pp. 97–111, 2002.

[10] A. Huete, K. Didan, T. Miura, and E. Rodriguez, "Overview of the radiometric and biophysical performance of the MODIS vegetation indices," *Remote Sens. Environ.*, vol. 83, pp. 195–213, 2002.

[11] D. P. Roy, J. S. Borak, S. Devadiga, R. E. Wolfe, M. Zheng, and J. Descloitres, "The MODIS land product quality assessment approach," *Remote Sens. Environ.*, vol. 83, pp. 62–67, 2002.

[12] M. A. Friedl, D. K. McIver, J. C. F. Hodges, X. Y. Zhang, D. Muchoney, A. H. Strahler, C. E. Woodcock, S. Gopal, A. Schneider, A. Cooper, A. Baccini, F. Gao, and C. Schaaf, "Global land cover mapping from MODIS: Algorithms and early results," *Remote Sens. Environ.*, vol. 83, pp. 287–302, 2002.

[13] J. Morisette, J. P. Privette, and C. O. Justice, "A framework for the validation of MODIS land products," *Remote Sens. Environ.*, vol. 83, pp. 77–96, 2002.

[14] B. Tan, J. Morisette, R. E. Wolfe, F. Gao, G. A. Ederer, J. Nightingale, and J. A. Pedelty, "Vegetation phenology metrics derived from temporally smoothed and gap-filled MODIS data," in *Proc. Int. Geoscience and Remote Sensing Symp. (IGARSS 2008)*, Jul. 2008, pp. 593–596.

[15] R. E. Wolfe, D. P. Roy, and E. Vermote, "MODIS land data storage, gridding, and compositing methodology: Level 2 grid," *IEEE Trans. Geosci. Remote Sens.*, vol. 36, no. 4, pp. 1324–1338, Jul. 1998.

[16] Z. Wan, Y. Zhang, Q. Zhang, and Z.-L. Li, "Validation of the land surface temperature products retrieved from Terra Moderate Resolution Imaging Spectroadiometer data," *Remote Sens. Environ.*, vol. 83, pp. 163–180, 2002.

[17] X. Zhang, M. Friedl, and C. B. Schaaf, "Global vegetation phenology from Moderate Resolution Imaging Spectroradiometer (MODIS): Evaluation of global patterns and comparison with *in situ* measurements," *J. Geophys. Res.*, vol. 111, no. Doi: 10.1029/2006JG000217, p. G04017, 2006.

[18] J. Levitt, *Responses of Plants to Enviromental Stresses*. New York: Academic Press, 1980.

[19] P. Jarvis and S. Linder, "Constraints to growth of boreal forests," *Nature*, vol. 405, pp. 904–905, 2000.

[20] W. Larcher, *Physiological Plant Ecology*. Heidelberg, Germany: Springer-Verlag, 1995.

[21] W. Larcher and H. Bauer, "Ecological significance of resistance to low temperature," in *Encyclopedia of Plant Physiology*, O. L. Lange, P. S. Nobe, C. B. Osmond, and H. Ziegler, Eds. Berlin, Germany: Springer-Verlag, 1981, vol. 12A, pp. 403–437.

[22] W. M. Jolly, R. Nemani, and S. Running, "A generalized, bioclimatic index to predict foliar phenology in response to climate," *Global Change Biol.*, vol. 11, no. Doi: 10.1111/j.1365-2486.2005.00930.x, pp. 619–632, 2005.

Bin Tan received the B.S. degree in geography and the M.S. degree in remote sensing and GIS from Peking University, Beijing, China, in 1998 and 2001, respectively, and the Ph.D. degree in geography from Boston University, Boston, MA, 2005.

From 2005 to 2007, he was a research associate with the Department of Geography, Boston University. He joined the NASA Goddard Space Flight Center, Greenbelt, MD, as a contractor from Earth Resources Technology (ERT), Inc. in 2007. His recent research interests include temporal data analysis, retrieving biophysical parameters, especially phenology metrics from satellite data, and modeling the vegetation change with high resolution satellite data.

Jeffrey T. Morisette is Assistant Center Director for Science and head of the Invasive Species Science Branch at the USGS Fort Collins Science Center. His current research is on the application of multi-resolution and time series satellite imagery to ecological and climate studies. Some of his current projects include invasive species habitat mapping in the National Parks and working with the U.S. National Phenology Network on land surface phenology research.

Robert E. Wolfe is a computer scientist in the Terrestrial Information Systems Branch within the Hydrospheric and Biospheric Sciences Laboratory at NASA's Goddard Space Flight Center. He has been involved in Earth remote sensing instruments, algorithms and data systems since 1980 when he received the B.S. degree from Bridgewater College, Bridgewater, VA.

After a decade of developing government and commercial remote sensing projects, he began working with the Moderate Resolution Imaging Spectroradiometer (MODIS) instruments, algorithms and data system in the early 1990s. His current areas of interest are focused on accurate satellite geolocation and developing data systems and algorithms for retrieving terrestrial biophysical and geophysical parameters. In 2004 he also became a NASA Science Team member for the joint NASA-NOAA-DOD National Polar-Orbiting Operational Environmental Satellite System (NPOESS) Preparatory Project (NPP) mission Visible Infrared Imager Radiometer Suite (VIIRS) instruments that are MODIS's follow-on operational instrument series. In 2006 he took on the role of Deputy Project Scientist for Data for the Earth Observing System (EOS) Terra satellite

and then joined the MODIS science team in 2007. He has over 60 publications (book chapters and scientific, technical, and symposia papers).

Dr. Wolfe is a member of the IEEE Geoscience and Remote Sensing Society and the American Geophysical Union.

Feng Gao (M'99) received the B.A. degree in geology and the M.S. degree in remote sensing from Zhejiang University, Hangzhou, China, in 1989 and 1992, respectively, the Ph.D. degree in geography from Beijing Normal University, Beijing, China, in 1997, and the M.S. degree in computer science from Boston University, Boston, MA, in 2003.

From 1992 to 1998, he was a Researcher with the Nanjing Institute of Geography and Limnology, Chinese Academy of Science. From 1998 to 2004, he was a Research Associate Professor with the Department of Geography and a Researcher in the Center for Remote Sensing, Boston University. He joined the NASA Goddard Space Flight Center, Greenbelt, Maryland, through a contract with Earth Resources Technology (ERT), Inc. in August 2004. His recent research interests include multi-sensor data fusion, remote sensing modeling, multi-temporal data analysis and vegetation biophysical parameters retrieving.

Dr. Gao is a member of the American Geophysical Union.

Gregory A. Ederer received the B.S. degree in computer science from the University of Virginia, Charlottesville, in 1982.

He currently works as a Chief Programmer/Analyst at Sigma Space Corporation on the Hydrospheric and Biospheric Sciences Support (HBSSS) contract for NASA Goddard Space Flight Center's Laboratory for Terrestrial Physics. He helped design and implement the laboratory's highly successful MODIS Data Processing System (MODAPS) for processing and archiving satellite imagery.

Joanne Nightingale received her undergraduate and doctoral degrees from the University of Queensland, Australia.

She is currently leading the Earth Observation Satellite (EOS) Land Product Validation program at NASA's Goddard Space Flight Center in Greenbelt, Maryland. Prior to joining NASA, she worked as a post-doctoral research fellow at Oregon State University and the University of British Columbia, Canada. Her research interests include assessing coupled soil-vegetation-atmosphere terrestrial processes and land surface phenology using satellite remote sensing and ecosystem/forest growth models.

Jeffrey A. Pedelty received the B.S. degree in physics from Iowa State University in 1981 and the Ph.D. in astrophysics from the University of Minnesota in 1988.

He has been at NASA's Goddard Space Flight Center since 1987 where he has supported a variety of Earth and space science missions (e.g., COBE, OSL, and Landsat 7) and performed basic and applied research in astrophysics, Earth science, image/signal processing and high performance computing. He is currently supporting the Landsat Data Continuity Mission (LDCM) as an onsite representative at Ball Aerospace and Technologies Corp. during the building and testing of the Operational Land Imager (OLI).

Dr. Pedelty is a member of the American Astronomical Society, the American Geophysical Union, and the American Association for the Advancement of Science.